Various scenarios for transition to thorium fuel cycle in the Single-fluid Double-zone Thorium Molten Salt Reactor (SD-TMSR)

O. Ashraf[a,b,*], Andrei Rykhlevskii[c], G. V. Tikhomirov[a], Kathryn D. Huff[c]

[a] *Laboratory of Engineering Computer Modeling in Nuclear Technologies, Institute of Nuclear Physics and Engineering, National Research Nuclear University MEPhI, Moscow, Russia, 115409*

[b] *Physics Department, Faculty of Education, Ain Shams University, Cairo, Egypt, 11341*

[c] *Dept. of Nuclear, Plasma, and Radiological Engineering, University of Illinois at Urbana-Champaign, Urbana, IL 61801, United States*

Abstract

Liquid-fueled Molten Salt Reactor (MSR) systems represent advances in safety, economics, sustainability, and proliferation-resistance. The MSR has been designed to operate in Th/^{233}U fuel cycle with ^{233}U used as start-up fissile material. Since ^{233}U does not exist in nature, it is required to examine other available fissile materials. This work investigated the fuel cycle and neutronics performance of the Single-fluid Double-zone Thorium-based Molten Salt Reactor (SD-TMSR) with different fissile material loadings at start-up: Low-enriched uranium (LEU) (19.79%), Pu mixed with LEU (19.79%), Pu reactor-grade (a mixture of plutonium isotopes chemically extracted from Pressurized Water Reactor (PWR) spent fuel with 33 GWd/tHM burnup), Transuranic elements (TRU) from Light Water Reactor (LWR) spent nuclear fuel (SNF) and finally ^{233}U. The MSR burnup routine provided by SERPENT-2 has been used to simulate the online reprocessing and refueling in the SD-TMSR. The effective multiplication factor, fuel salt composition evolution and net production of ^{233}U have been studied in the present work. The results show that the continuous flow of Pu reactor-grade helps in transition to thorium fuel cycle within a relatively

*Corresponding Author

Email address: osama.ashraf@edu.asu.edu.eg oabdelaziz@mephi.ru (O. Ashraf)

short time (≈ 4.5 *years*) compared to 26 *years* for ^{233}U start-up fuel. Finally, using TRU as initial fissile materials shows the possibility of operating the SD-TMSR for a long period of time (≈ 40 years) without any external feed of ^{233}U.

Keywords: MSR, thorium fuel cycle, transmuter, burner, online reprocessing, Monte carlo code

1. Introduction

The Generation IV International Forum (GIF) has defined eight technology goals for the next generation nuclear systems. These goals have been defined in four broad areas: safety and reliability, economics, sustainability, non-proliferation and physical protection [1]. Molten Salt Reactors (MSRs) have many advantages that consistent with GIF's goals, for example, liquid fuel, inherent safety, online reprocessing and refueling, excellent neutron economy and operation under ambient pressure [2, 3]. Therefore, in 2002 the MSR has been chosen as one of the promising reactors by this forum [1, 4]. In the MSR, the fuel supposed to be in the form of liquid dissolved in molten salt (e.g., LiF or NaCl). This liquid fuel salt (e.g., LiF-BeF_2-ThF_4-$^{233}UF_4$) constantly circulates through the core and allows transferring fission heat.

The Single-fluid Double-zone Thorium-based Molten Salt Reactor (SD-TMSR-2,250 MWth) was introduced by the Chinese Academy of Sciences (CAS) [5]. The SD-TMSR is a graphite-moderated thermal-spectrum MSR. In the SD-TMSR the fissile and fertile elements are integrated into the same salt. In addition, the active core is divided into two zones, the radius of the fuel channels in the outer zone is modified to be larger than the radius of the fuel channels in the inner zone to improve the breeding ratio [6, 5].

Basically, the MSR has been designed to apply the Th/^{233}U fuel cycle [7, 6, 8, 3]. Hence, the fertile isotope ^{232}Th is converted to the fissile isotope ^{233}U, an isotope that is not exist in nature. Therefore it is required to examine available fissile materials (e.g., ^{235}U and Pu) to replace the ^{233}U in the startup

fuel [9, 10]. The thorium fuel cycle transition can be achieved after reaching the doubling time[1] of ^{233}U.

Betzler, et al. discussed the simulation of the start-up of a MSBR unit cell with LEU (19.79%) and Pu from Light Water Reactor (LWR) spent fuel (SF) as initial fissile materials [9]. They concluded that the plutonium vector extracted from LWR SF serves as the best alternative source to ^{233}U thanks to the highest ratio of fissile isotopes [9]. Zou, et al. introduced two approaches for the thorium fuel cycle transition in Thorium-based Molten Salt Reactor (TMSR): in-core transition and ex-core transition. In the former way, the TMSR is launched with existing fissile material and thorium as a fertile material, then the bred ^{233}U from thorium is rerouted into the core for criticality. In contrast, the latter way tends to store the bred ^{233}U out of the core until there is enough amount to start a new TMSR [10]. Meanwhile, Zou, et al. studied the transitioning to thorium fuel cycle in a small modular Th-based molten salt reactor (smTMSR) using TRUs as startup fuel. They concluded that the transition to thorium fuel cycle can be achieved in thermal smTMSR with a proper fuel fraction [11]. Heuer, et al., discussed the transition characteristics of the Molten Salt Fast Reactor (MSFR) under different launching scenarios (e.g., enriched uranium and TRU), they concluded that starting the Thorium fuel cycle is feasible while closing the current fuel cycle and adopting stockpile incineration in MSRs for optimizing the long-term waste management [12].

Indeed, there are various researches that revolve around starting the MSRs with fissile materials alternative to ^{233}U. Many of these researches focus on the fast-spectrum MSRs [13, 14, 12, 15], while little focus on thermal-spectrum MSRs [9, 11, 10]. Nevertheless, starting the Single-fluid Double-zone Thorium-based Molten Salt Reactor (SD-TMSR) with other fissile materials (except ^{233}U) not found in the literature. Therefore, the main object of the present paper is to discuss the simulation of the operation of SD-TMSR for a long period of time (60 years) with different initial fissile materials and without any external feed

[1] Time required to produce enough amount of ^{233}U to trigger a new SD-TMSR.

of ^{233}U to achieve the thorium fuel cycle transition. To do that, we investigate five types of initial fissile materials based on Low-enriched uranium (LEU), Pu mixed with LEU, Pu reactor-grade, Transuranic elements (TRU) from LWR SF and ^{233}U [16]. Moreover, two different feed mechanisms are used as follows:

- Continuous feed flow of thorium from Th stockpile and ^{233}U from `Pa-decay tank`[2], where the removal rate of ^{233}Pa = feed rate of ^{233}U. [9].
- Continuous injection of Heavy Metal (HM) (excluding Th) and simultaneously feed of all or part of produced ^{233}U from `Pa-decay tank`.

All calculations presented in the present paper were performed using SERPENT-2 version 2.1.30. We used the MSR burnup routine provided by SERPENT-2 to simulate continuous online reprocessing and refueling. SERPENT-2 uses an internal calculation routine for solving the set of Bateman equations describing the changes in the material compositions caused by neutron-induced reactions and radioactive decay [24]. Additionally, SERPENT-2 allows us to conduct the burnup calculations on computer clusters with multiple cores using distributed-memory MPI parallelization.

This present paper is organized as follows: after an introduction about MSR systems, the model description is discussed in section 2. Methodology and tools is descried in section 3. Extraction and feed mechanisms are addressed in section 4. Section 5 focuses on the results and discussion. Finally, section 6 highlights the conclusions.

2. Model description

2.1. Geometry

The SD-TMSR design model was introduced by the CAS during the strategic project "Future Advanced Nuclear Energy − Thorium-based Molten Salt Reactor System (TMSR)" in 2011 [5, 17, 18, 19]. The design of SD-TMSR is inspired

[2] An imaginary tank used to store protactinium extracted from the core.

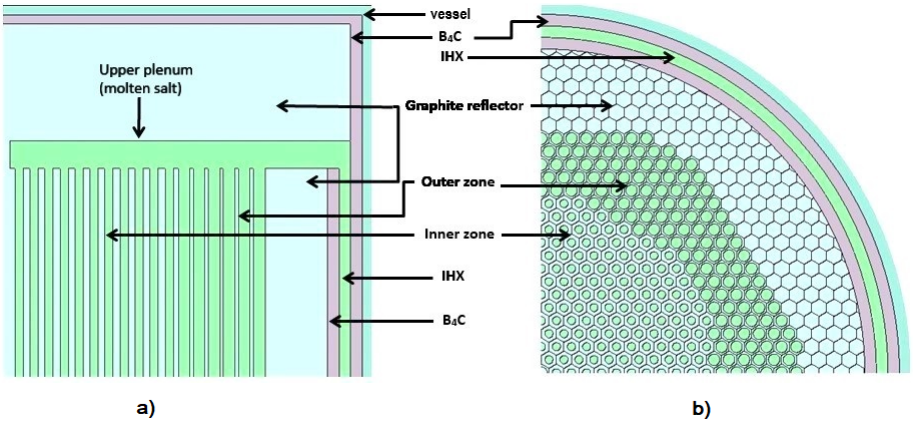

Figure 1: The quarter-core model configuration of the SD-TMSR a) Longitudinal view b) Cross-sectional view at the horizontal midplane.

by Molten Salt Breeder Reactor (MSBR) [20] after some modification in the geometry to control the positive temperature coefficient in MSBR. The SD-TMSR model is described deeply in [5]. Figure 1 illustrates the quarter-core model configuration of the SD-TMSR. The active zone is a right cylinder with height and diameter equal to 460 cm. Assemblies of graphite[3] hexagonal prisms fill the core. The side length of the graphite hexagonal prism was optimized in [5] and found to be 7.5 cm. The liquid fuel circulates continuously through the fuel channels that pierces the graphite hexagonal prisms. The active zone is divided into two different zones to enhance Th-U breeding performance. The radius of the fuel tubes in the outer zone is 5 cm and the radius of the fuel tubes in the inner zone is 3.5 cm. Moreover, axial and radial reflectors from graphite surround the active zone to maximize neutron flux. The core is surrounded by B_4C cylinder that acts as a shield against heat and neutrons radiation. Another Ni-based (hastelloy N) cylinder surrounds the whole core and provides structure and heat protection. The main characteristics of the SD-TMSR are listed in Table 1.

[3]We choose graphite density of 2.3 g/cm^3, to validate our results against results in the literature [5, 6].

Table 1: The main characteristics of the SD-TMSR [5]

Thermal power, MW_{th}	2,250
Fuel salt components	LiF-BeF_2-$(HM)F_4$
Fuel composition, mole%	70-17.5-12.5
^{7}Li enrichment, %	99.995
Fuel temperature, K	900
Fuel density at 900 K, g/cm^3	3.3
Fuel dilatation coefficient, g/(cm^3 .K)	-6.7$\times 10^{-4}$
Graphite density, g/cm^3	2.3
B_4C density, g/cm^3	2.52
^{10}B enrichment, %	18.4
Core diameter, cm	460
Core height, cm	460
Side length of the graphite hexagonal prism, cm	7.5
Inner radius, cm	3.5
Outer radius, cm	5
Ratio of molten salt and graphite in the inner zone	0.357
Ratio of molten salt and graphite in the outer zone	1.162
Fuel volume, m^3	52.9

Table 2: Reactor-grade plutonium vector [21]

^{238}Pu	^{239}Pu	^{240}Pu	^{241}Pu	^{242}Pu
1.3	60.3	24.3	9.1	5

Table 3: TRU vector (%) [16]

^{237}Np	^{238}Pu	^{239}Pu	^{240}Pu	^{241}Pu	^{242}Pu	^{241}Am	^{243}Am	^{244}Cm	^{245}Cm
6.3	2.7	45.9	21.5	10.7	6.7	3.4	1.9	0.8	0.1

2.2. Fuel composition

The general composition of the liquid fuel salt in this work is 70LiF - 17.5BeF_2 - 12.5(HM)F_4 mole%, where HM is the heavy metal (i.e. thorium + different fissile materials). As previously mentioned, the aim of this paper is to simulate the operation of SD-TMSR for a long period of time (60 years) with different initial fissile materials and without any external feed of ^{233}U. Therefore, five different types of initial fissile materials based on LEU, Pu, and TRU from LWR SF are investigated as follows:

(1)low-enriched uranium (LEU) (19.79%);

(2)Pu mixed with LEU (19.79%);

(3)Pu reactor-grade [21];

(4)transuranic (TRU) elements from LWR SF [16];

(5)and ^{233}U for comparison purpose.

The reactor-grade plutonium and TRU vector (%) are summarized in Table 2 and 3, respectively.

The isotopic compositions of plutonium recovered from the spent fuel composition of commercial LEU Pressurized Water Reactor (PWR) that has released 33 GWd/t fission energy and has been cooled for 10 $years$ before reprocessing [22, 21]. As well, the isotopic compositions of TRU have been taken from the SF of UOX PWR (after one use and without multi-recycling) with 60 GWd/t

Table 4: Composition of startup fuel mole%

Molecule	LEU (19.79%)	Pu mixed with enriched U (19.79 wt-%)	Pu reactor-grade	TRU	^{233}U
LiF	70	70	70	70	70
BeF_2	17.5	17.5	17.5	17.5	17.5
ThF_4	8.25	7.5	10.75	8.65	12.3
UF_4	4.25	4.75			0.2
PuF_3		0.25	1.75		
$TRUF_3$				3.85	

burnup, and after 5 *years* cooling [16]. The molar composition of startup fuel for all five cases is listed in Table 4. Meanwhile, the corresponding initial nuclei inventories with different types of fuel are tabulated in Table 5.

3. Methodology and tools

Simulation of Liquid-fueled Molten Salt Reactor (MSR) systems requires computational software that must support online fuel salt reprocessing and refueling [23]. In this work, SERPENT-2 version 2.1.31 beta[4] [24] is used to simulate the full-core of the SD-TMSR with different types of initial fuel. The extension of SERPENT code accounts for continuous online reprocessing and refueling [25]. Meanwhile, ENDF-VII.0 cross-section library is adopted for all calculations. The results demonstrate full-core runs of $12.5E+06$ neutron history per depletion step. The full burnup time of the SD-TMSR was 60 years with statistical error in k_{eff} equal to $\pm$ 36 *pcm*. The online extraction of Fission

[4]SERPENT-2 is a Three Dimensions (3D) continuous energy Monte Carlo neutron transport and burn-up code.

Table 5: Initial nuclei inventories (in grams) of the SD-TMSR with different types of fuel.

Molecule	LEU (19.79%)	Pu mixed with enriched U (19.79%)	Pu reactor-grade	TRU	^{233}U
^{232}Th	6.24E+07	4.67E+07	6.75E+07	5.44E+07	7.69E+07
^{233}U					1.30E+06
^{235}U	3.17E+06	6.01E+06			
^{238}U	1.28E+07	2.43E+07			
^{237}Np				1.58E+06	
^{238}Pu		1.60E+04	1.13E+05	6.78E+05	
^{239}Pu		9.59E+05	6.76E+06	1.15E+07	
^{240}Pu		3.99E+05	2.82E+06	5.40E+06	
^{241}Pu		1.60E+05	1.13E+06	2.69E+06	
^{242}Pu		6.39E+04	4.51E+05	1.68E+06	
^{241}Am				8.53E+05	
^{242}Am					
^{243}Am				4.77E+05	
^{244}Cm				2.01E+05	
^{245}Cm				2.51E+04	
Total mass of HM without ^{232}Th	1.60E+07	3.20E+07	1.13E+07	2.51E+07	1.30E+06

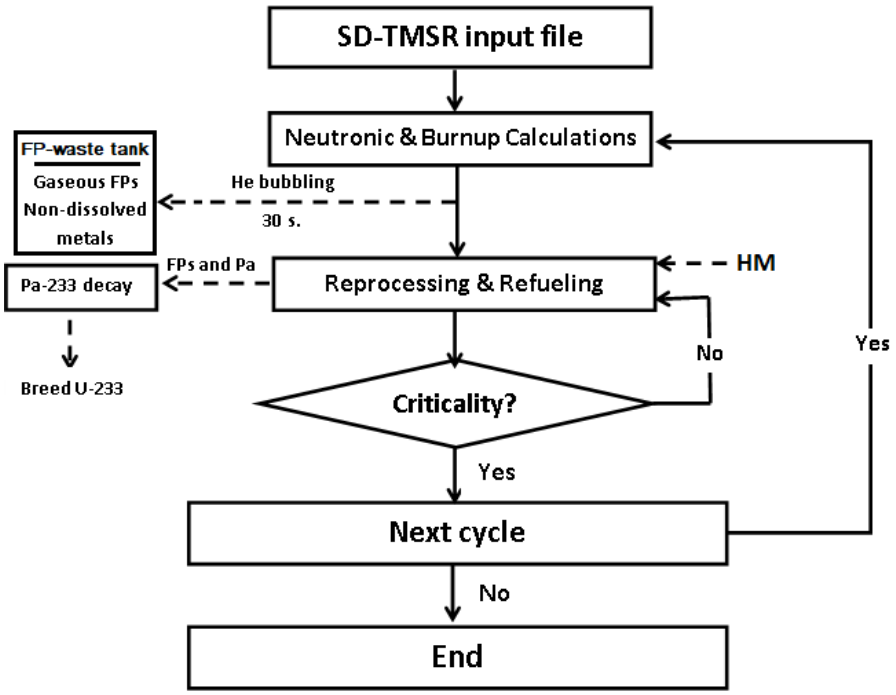

Figure 2: Flow chart of the calculation procedures.

Products (FPs) and noble gases provides many benefits for MSRs. For example, it would reduce the fissile inventory required to achieve criticality and improve the breeding ratio. Figure 2 shows a flow chart of the calculation steps.

As shown in Figure 2, after launched the input file, an advanced matrix exponential solution based on the Chebyshev Rational Approximation Method (CRAM) [26] used to solve the Bateman equation. Then, the system extracted gaseous FPs and other materials (non-dissolved metals, lanthanides, and soluble metals except Pu) in a proper time. This can be done by set the flow rate of gaseous FPs and other materials from the fuel to the `FP-waste tank`[5]. Specifically, protactinium was removed from the fuel with a certain flow rate into the

[5] An imaginary tank used to store the gaseous FPs and the other materials (non-dissolved metals, lanthanides, and soluble metals except protactinium).

external tank, `pa-decay tank`, to decay and produce ^{233}U[6]. The produced ^{233}U is used as a fresh fissile fuel and the residual ^{233}U is the net production of ^{233}U. The MSR burnup routine provided by SERPENT-2 allows changes the flow rates ($mflow$) of the isotopes during reactor operation [25]. The mass of the fissile and fertile materials needed to achieve criticality is calculated at the end of the cycle. Then, this mass is added to the core at the beginning of the cycle by a certain flow rate.

4. Feed and extraction rates

In the present work, two different feed mechanisms are used. The first mechanism allows continuous feed flow of thorium and ^{233}U from `pa-decay tank`. In contrast, the second mechanism adopts continuous feed flow of (Heavy Metal (HM) except for Th) + all or part of ^{233}U from `Pa-decay tank`.
The fission products act as poisons in the MSRs; they negatively impacting the reactivity. Therefore, FPs must be extracted during reactor operation. Consider T_r as the time during which the total fuel salt is reprocessed and dN_e as the amount of particular element e with inventory N_e that the MSR extracts during time dt; thus [6]

$$\frac{dN_e}{dt} = N_e \frac{\varepsilon_e}{T_r}, \tag{1}$$

where ε_e is the removal efficiency. Equation 1 gives the removal constant λ_e $[s^{-1}]$ (the rate at which the material is removed), where $\lambda_e = \varepsilon_e / T_r$. The removal constant λ_e of gaseous and other fission products is precisely calculated and summarized in Table 6. The effective reprocessing time for the gaseous FPs and non-dissolved metals was set to 30 seconds (removal constant $\lambda_e = -0.0333\ s^{-1}$), because such elements must be extract promptly and continuously via He bubbling system. In contrast, extracting the soluble FPs, lanthanides, and protactinium can be done by the chemical reprocessing (i.e. fluorination

[6]The ^{233}Pa is removed and left to decay into ^{233}U with $\tau_{1/2} \approx 27\ d$.

and reduction reaction). Therefore, the system reprocesses a specific amount of fuel salt daily. In the present work, the effective extraction time for soluble FPs is ≈10.59 days ($\lambda_e = -1.092 \times 10^{-6}\ s^{-1}$), which is equivalent to 5 m^3/d of chemical reprocessing rate [6, 5]. The effective feed rates of the heavy metals (HM) are changed during reactor operation to conserve the total fuel mass and criticality.

Table 6: The reprocessing table.

Reprocessing group	**Element**	**Reprocessing time**	**Removal constant λ_e $[s^{-1}]$**
Gaseous FPs and non-dissolved metals	H, He, N, O, Ne, Ar, Kr, Nb, Mo, Tc, Ru, Rh, Pd, Ag, Sb, Te, Xe, Lu, Hf, Ta, W, Re, Os, Ir, Pt, Au and Rn.	30s	-3.333E-02
Lanthanides and other soluble FPs	Zn, Ga, Ge, As, Se, Br, Rb, Sr, Y, Zr, Cd, In, Sn, I, Cs, Ba, La, Ce, Pr, Nd, Pm, Sm, Eu, Gd, Tb, Dy, Ho, Er, Tm and Yb.	10.599 d (5 m^3/d)	-1.092E-06
Protactinium	Pa	10.599 d (5 m^3/d)	-1.092E-06

5. Results and discussion

5.1. Thorium feed mechanism

The first mechanism adopts continuous feed flow of external thorium and ^{233}U from `Pa-decay tank`. Hereinafter the first mechanism will be mentioned as the thorium feed mechanism. The molar fraction of the heavy metal in the initial fuel was kept constant and equal to 12.5 mole% for all cases. Besides, the initial

fissile material fraction was increased for the five fuel salt compositions until the SD-TMS reactor was sufficiently critical at the Beginning Of Life (BOL). Figure 3 illustrates the change of the effective multiplication with Effective Full-Power Years (EFPY) for the thorium feed mechanism. As shown in Figure 3, the effective multiplication factor (k_{eff}) decreases sharply during the first 25 years of reactor operation for the first four cases. k_{eff} decreases as a result of depletion of the initial fissile materials and generation of the neutron poisons (FPs). Thus, the reactor becomes subcritical within a relatively short time ($\approx 4\ years$ in the TRU case and $\approx 12\ years$ in the Pu reactor-grade case). The amount of ^{233}U generated in the SD-TMSR is not enough to conserve the reactor criticality and overcome the neutron absorption in the initial fertile isotopes. Nevertheless, the continuous feed flow of thorium and ^{233}U helps to operate the SD-TMSR for a long period of time (the U-233 case). Additionally, the initial molar fraction in the LEU and Pu reactor-grade cases was increased more (see Figure 3) to counteract the absorption of neutrons in the non-fissile heavy metals added with the initial fuel salt. But k_{eff} still decreases below 1.0, as a result of increasing the non-fissile heavy metals in the initial fuel [9].

5.2. Non-thorium feed mechanism

The second mechanism allows continuous feed flow of ^{233}U from `Pa-decay tank` and Heavy Metal except for Th. Hereinafter the second mechanism will be mentioned as the non-thorium feed mechanism. Figure 4 shows the change of the effective multiplication during 60 EFPY of reactor operation for the non-thorium feed mechanism. As shown in Figure 4, the SD-TMS reactor was sufficiently critical at the Beginning Of Life (BOL). Both Pu reactor-grade and TRU case show promising results relative to the other two cases (i.e. LEU and Pu+LEU). For the Pu reactor-grade fuel salt, the amount of ^{233}U generated in the SD-TMSR in addition to the external feed flow of Pu are sufficient to maintain the reactor criticality and overcome the neutron absorption in the initial non-fissile isotopes. This may be attributed to the fact that the spectrum in the Pu reactor-grade initial core is hardened that is more thorium is being

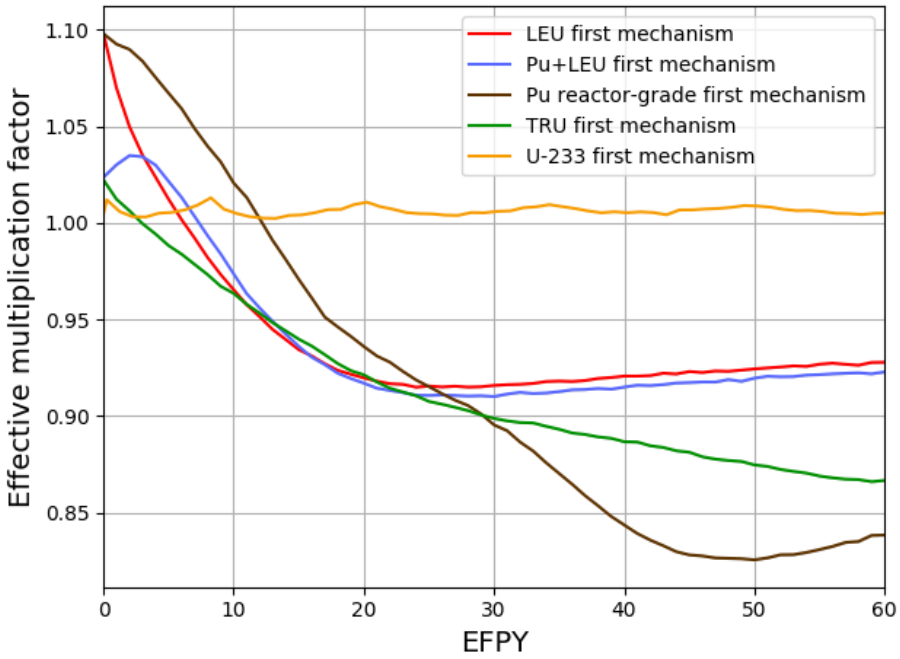

Figure 3: The change of the effective multiplication factor during 60 EFPY of reactor operation for thorium feed mechanism (confidence interval $\pm\sigma$ is shaded).

converted to ^{233}U. For the TRU fuel salt, the amount of ^{233}U and the external feed flow of TRU is barely enough to operate the reactor for a long period of time ($\approx 40\ years$) without any external feed of ^{233}U. Nevertheless, k_{eff} decreases with the burnup because the Minor Actinides[7] (MA) accumulating in the core as a result of continuous TRU feed. As shown in Figure 4, the LEU and Pu+LEU fuel are less attractive for non-thorium feed mechanism. The continuous LEU feed increases the amount of fertile ^{238}U and consequently, reduces the feasibility of such fissile materials. The continuous feed of ^{233}U without ^{232}Th will lead to supercritical reactor, thus the ^{233}U case is excluded from non-thorium feed mechanism.

According to the k_{eff} results, Pu reactor-grade and TRU fissile materials are selected and discussed in the following.

5.3. Pu reactor-grade, TRU, and ^{233}U initial fuel

In this section, the simulation of the SD-TMSR with Pu reactor-grade and TRU fissile materials is discussed. Besides, the ^{233}U case is listed for comparison. Figure 5 demonstrates the dynamics of heavy metal refill rate during 60 EFPY of SD-TMSR operation. The heavy metal refill rate was adjusted to maintain; the reactor criticality and total fuel mass almost constant[8] during the reactor operation. In ^{233}U case, the mean values of ^{233}U and ^{232}Th refill rate are 1.77 and 2.21 kg/d, respectively. As well, in the Pu reactor-grade case, the mean values of ^{233}U and Pu refill rate are 0.75 and 2.75 kg/d, respectively. In the TRU case, the mean values of ^{233}U and TRU refill rate are 0.90 and 2.0 kg/d, respectively.

Figure 6 and 7 describe the evolution of important isotopes for ^{233}U, Pu and TRU cases respectively. From Figure 6, the mass of Pa in the fuel salt is almost constant and reaches 17.8 kg at the end of the operation time. In addition, the mass of Minor Actinides (MA) increases with time; however, by applying online

[7] In the present work, the Minor Actinides (MA) include Np, Am and Cm.

[8] The variation of the total fuel mass is less than 0.1%

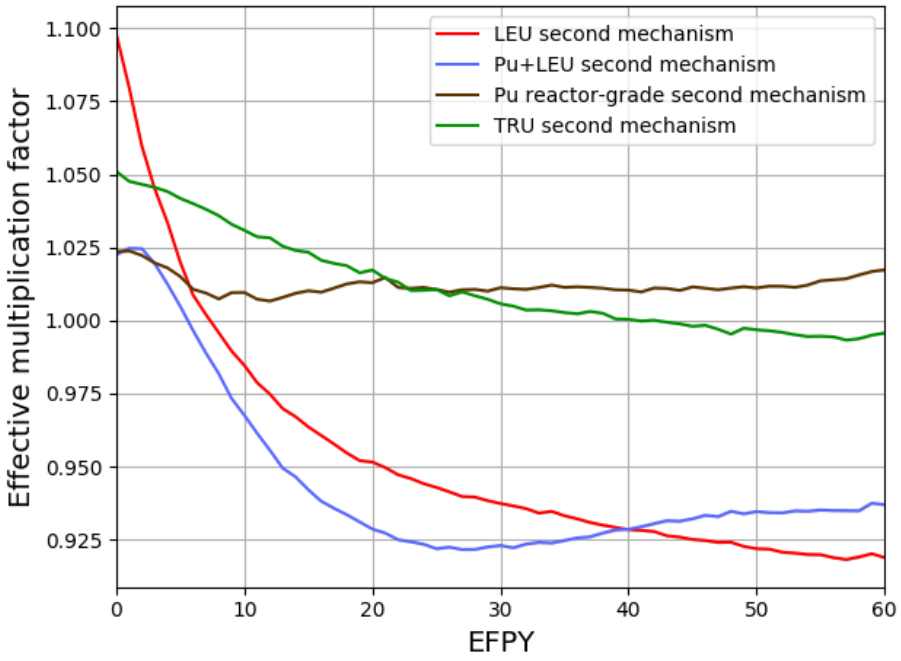

Figure 4: The change of the effective multiplication factor during 60 EFPY of reactor operation for non-thorium feed mechanism (confidence interval $\pm\sigma$ is shaded).

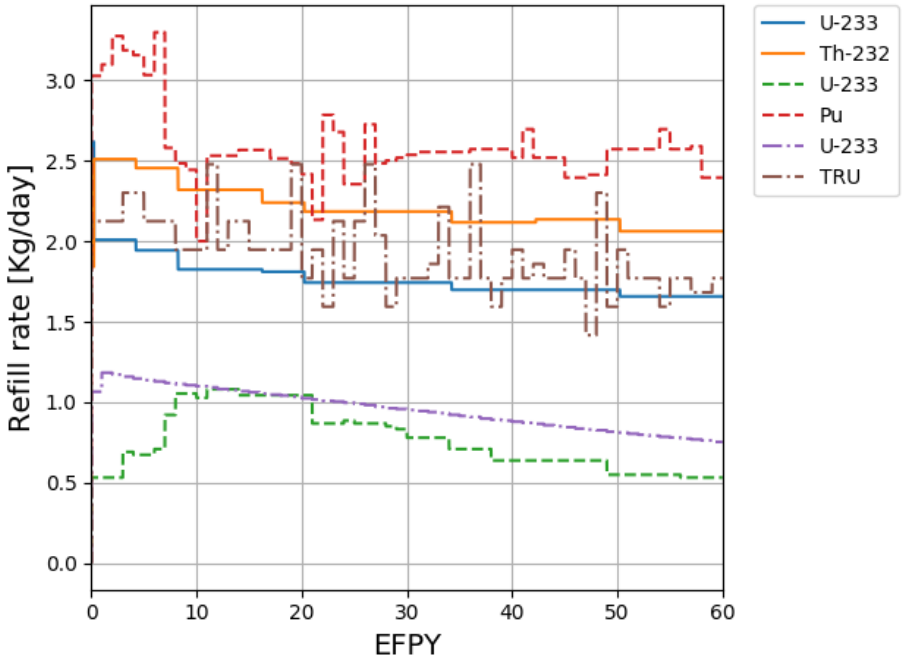

Figure 5: Dynamics of heavy metal refill rate during 60 EFPY of reactor operation. Solid lines for ^{233}U case, dashed lines for Pu reactor-grade case, and dotted lines for TRU case.

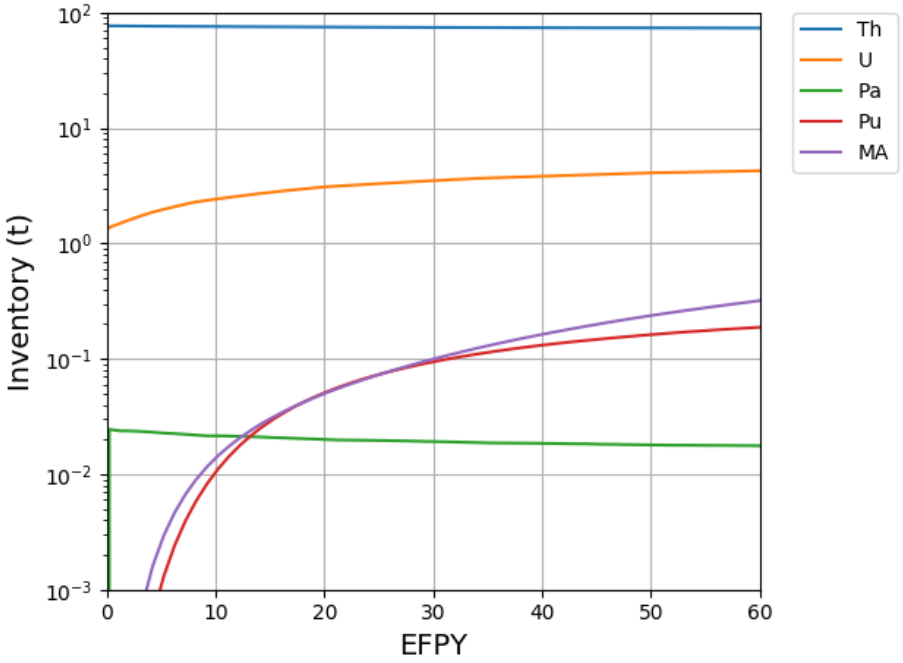

Figure 6: Evolution of the important nuclides inventories for ^{233}U case (MA involves Np, Am, Cm).

reprocessing, its value remains relatively low. As well, the total mass of Pu increases with burnup. The level of Pu in the fuel correlates with the mass of the MA, and Pu. MA need more time to reach equilibrium. The total mass of U increases with burnup and reaches equilibrium after ≈ 27 *years*. As shown in Figure 6, refueling the core with Th helps maintain an almost constant inventory throughout the full operation time.

The Pa extraction time was adjusted to be 30 seconds for Pu and TRU cases to avoid poisoning the core. Therefore, Figure 7 shows that the mass of Pa in the fuel for Pu and TRU cases is relatively low when compared to the ^{233}U case. Major isotopes for the three cases reaches the equilibrium state after ≈ 30 *years* (see Figure 6 and 7).

Figure 8 illustrates the variation of thorium mass in the fuel salt for ^{233}U, Pu reactor-grade and TRU cases, respectively. In ^{233}U case, we apply the thorium

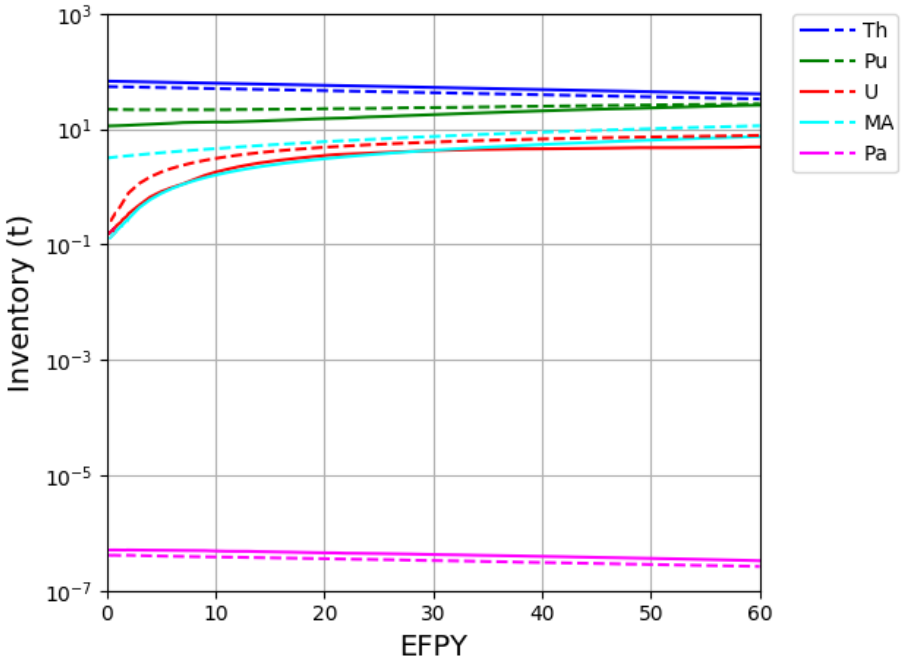

Figure 7: Evolution of the important nuclides inventories for Pu reactor-grade case (solid lines) and for TRU case (dashed lines).

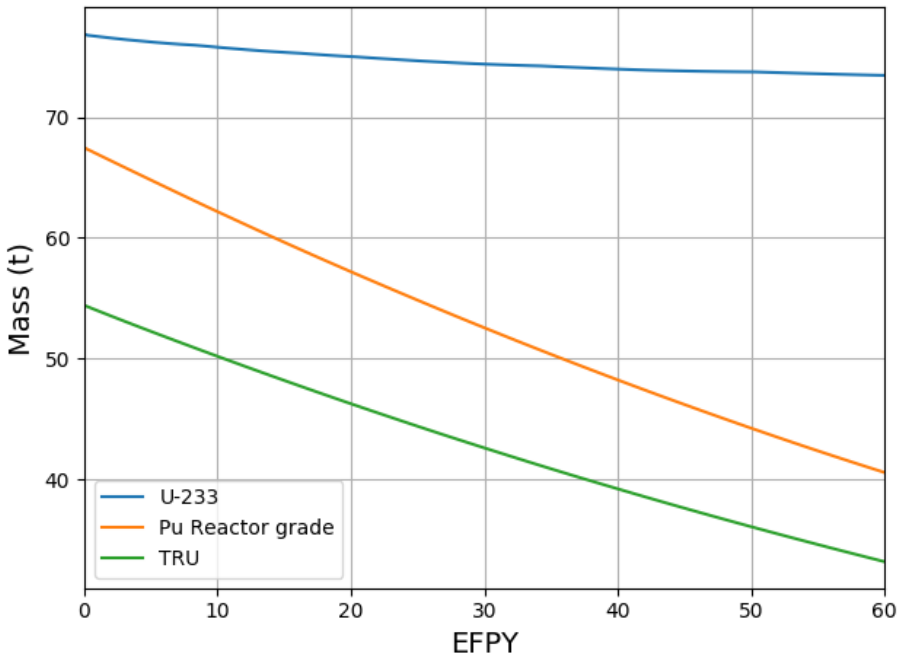

Figure 8: The variation of thorium mass in the fuel salt for ^{233}U, Pu reactor-grade and TRU cases, respectively.

feed mechanism, thus thorium mass decreases by only 3.2 % at the end of operation time (60 years). In contrast, thorium mass decreases significantly in Pu and TRU cases according to the non-thorium feed mechanism. Thorium mass decreases by 39.2 % and 37.96 % in Pu reactor-grade and TRU cases, respectively. The more decreasing in thorium mass, the more effective utilization of thorium fuel cycle. Consequently, the Pu reactor-grade initial fuel may help to utilize thorium fuel cycle more effective.

Figure 9 demonstrates the mass of ^{233}U in the fuel salt for ^{233}U, Pu reactor-grade and TRU cases, respectively. One can see that the mass of the ^{233}U reaches the equilibrium state after ≈ 30 *years*. Meanwhile, the amount of ^{233}U is sufficient to maintain criticality in the three cases.

In the non-thorium feed mechanism, the SD-TMSR is continuously refueled for criticality, which increases the Pu proportion in the molten salt. According

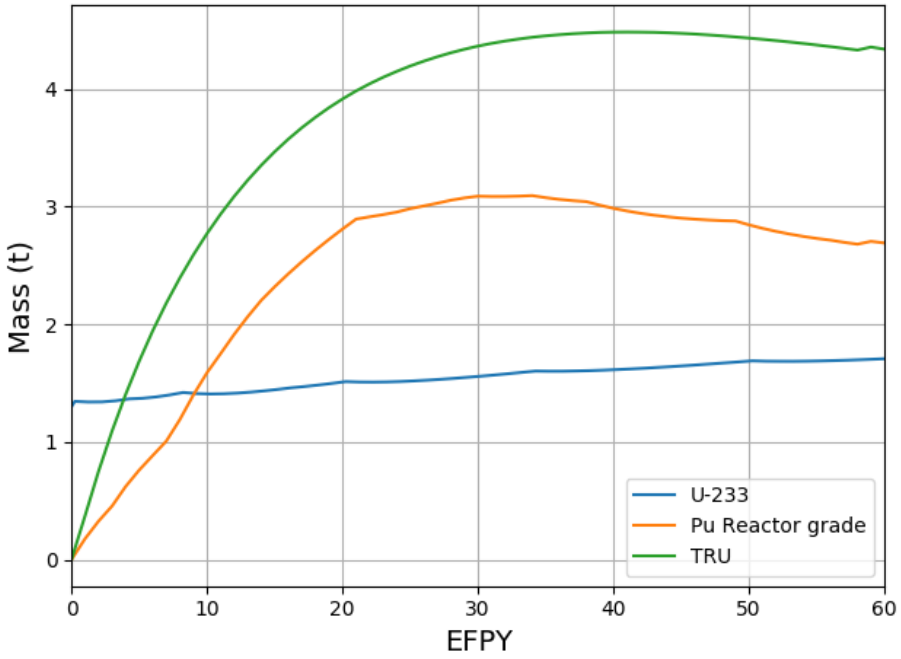

Figure 9: Mass of ^{233}U in the fuel salt for ^{233}U, Pu reactor-grade and TRU case, respectively.

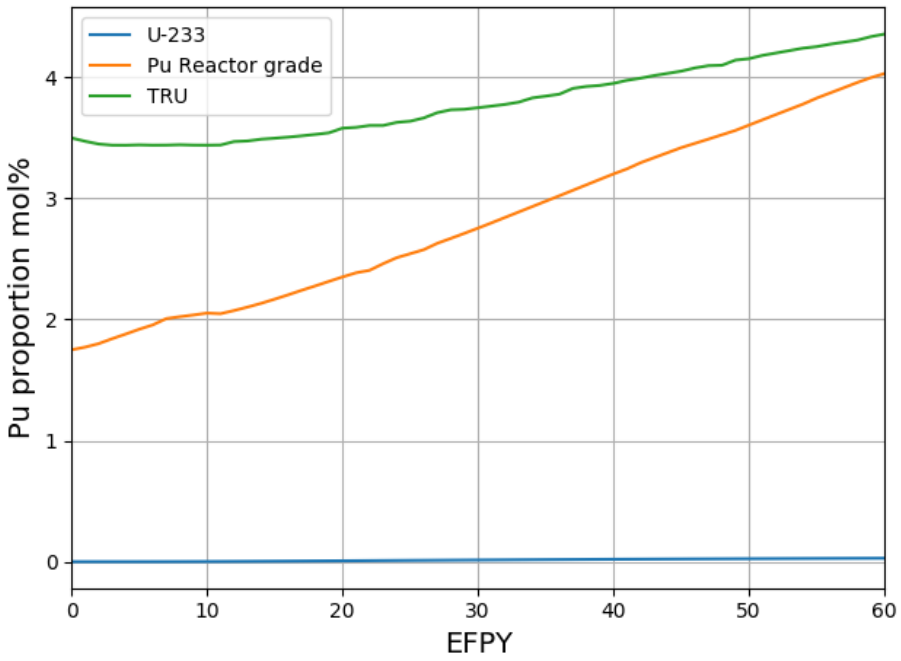

Figure 10: The Pu proportion in the fuel salt (mole%).

to the literature, the limit of Pu solubility in the FLiBe salt is ≈ 4.0 % [27, 28]. Figure 10 represents the Pu proportion in the fuel salt (mole%). In ^{233}U and Pu reactor-grade cases, the Pu proportion increases slightly but still below its solubility limit. On the other hand, the Pu proportion in the molten salt loaded by TRU increases with operation time and reaches the Pu solubility limit after ≈ 40 *years*. This issue may be solved by increasing the reactor operation temperature and or reducing the HM initial inventory [10].

Figure 11 demonstrates the net production of ^{233}U as a function of burnup. In TRU case, the net production of ^{233}U is almost zero, nevertheless, the reactor becomes subcritical after 40 *years* of operation. In ^{233}U and Pu reactor-grade cases, the net production of ^{233}U increases with burnup and reaches about 1.77 t and 10 t, respectively at the end of operation lifetime. It worth noting that thorium feed mechanism is applied in ^{233}U case, while, non-thorium feed mechanism is adopted in Pu reactor-grade cases. As shown in Figure 11, after 26

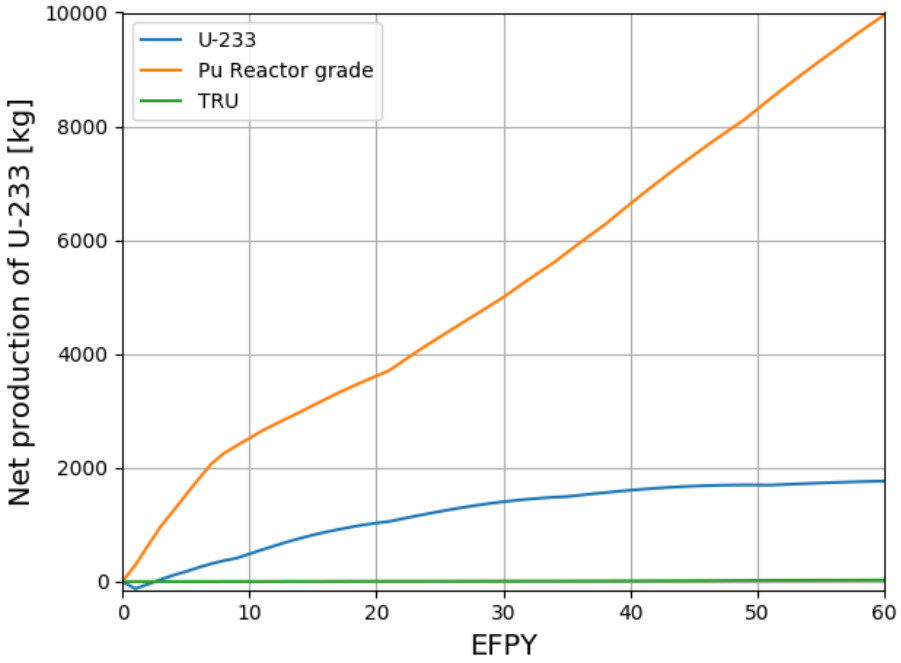

Figure 11: Net production of ^{233}U during burn-up period (60 EFPY).

years the net production of ^{233}U reaches 1.3 t; this is sufficient to start-up another SD-TMSR. Similarly, one can see that the same amount of ^{233}U (i.e. 1.3 t) can be achieved after $\approx$ 4.5 *years* if we applied the non-thorium feed mechanism on the SD-TMSR that initially loaded by Pu reactor-grade alternative to ^{233}U. In addition, Figure 11 also shows that the net production of ^{233}U during the first 455 days is negative, thus about 175.28 kg of ^{233}U must be added during this period. In conclusion, the thorium fuel cycle transition can be achieved by selecting the proper feed mechanism and initial fissile material.

5.4. Neutron spectrum

Figure 12 represents the neutron flux per unit lethargy for full-core SD-TMSR model in the energy range from 10^{-8} to 10 MeV for the ^{233}U, Pu reactor-grade, and TRU started case. In ^{233}U case, at the EOL, the neutron spectrum is harder than at BOL due to the accumulation of the Pu and other strong thermal

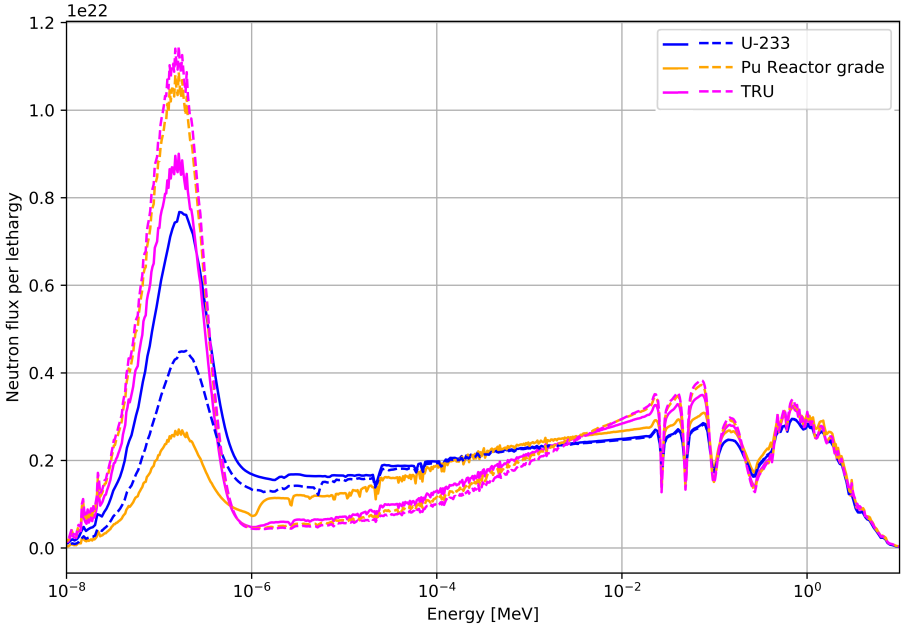

Figure 12: The neutron flux energy spectrum at BOL (solid lines) and EOL (dashed lines) for ^{233}U, Pu reactor-grade, and TRU case.

neutron absorbers in the fuel salt. For Pu reactor-grade and TRU cases, during the reactor operation, the fissile Pu is depleted and the ^{233}U becomes the major fissile isotope (see Figure 9), the neutron spectrum softens and becomes similar to a thermal spectrum of the TMSR.

290 The comparison between the two feed mechanisms with different types of initial fuel is listed in Table 7.

Table 7: Comparison between the two feed mechanisms for the five different types of initial fuel.

Feed mechanism \ Initial fuel	LEU (19.79%)	Pu mixed with enriched U (19.79 wt-%)	Pu reactor-grade	TRU	^{233}U
Thorium feed mechanism	Not work	Not work	Not work	Not work	Work
Non-thorium feed mechanism	Not work	Not work	Work well with positive net production of ^{233}U	Work for 40 *years* with net production of ^{233}U = zero	Not examine (supercritical reactor)

5.5. Neutron flux

Figures 13, 14 show the radial distribution of fast (energy range between 0.625 eV and 20 MeV) and thermal (energy range between 10^{-5} eV and 0.625 eV) neutron flux for three different initial fissile materials in the fuel salt (^{233}U, reactor-grade plutonium, TRU) at startup and at equilibrium (after ≈ 30 years of operation). Actinides evolution and poisonous fission product accumulation for various initial fissile compositions demonstrated the different effects on the SD-TMSR neutronics performance. For the Th/^{233}U, the thermal neutron flux is suppressed at the equilibrium because fissile ^{233}U in the core is being substituted with heavier fissile actinides: ^{235}U, ^{239}Pu, and ^{241}Pu. This is in good agreement with results in the literature [7, 29].

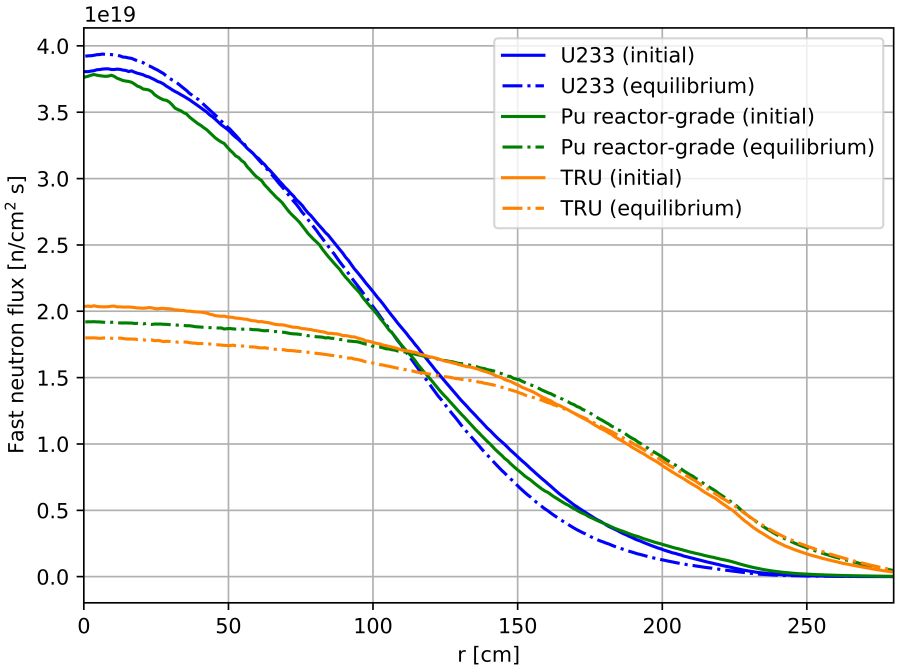

Figure 13: Radial fast neutron flux distribution for 3 different initial fuel salt compositions at startup and equilibrium (the fast flux confidence interval $\pm\sigma < 2.5\%$ for all cases).

Opposite behavior was observed for the Pu reactor-grade and TRU cases. For these cases, the thermal neutron flux is increasing during operation while

fast neutron flux is decreasing. Fissile plutonium nuclides (generate relatively hard spectrum) from initial fuel salt composition is gradually substituted with the ^{233}U (generates relatively soft spectrum), produced from the fertile ^{232}Th. During reactor operation, the ^{233}U becomes primary fissile isotope, which leads to the neutron spectrum softening of the reactor.

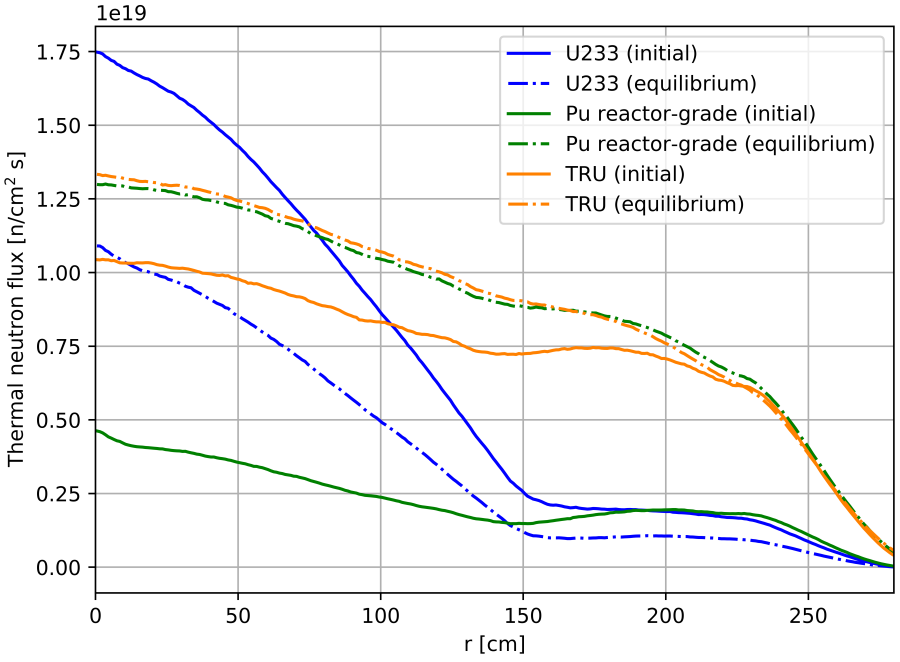

Figure 14: Radial thermal neutron flux distribution for 3 different initial fuel salt compositions at startup and equilibrium (the thermal flux confidence interval $\pm\sigma < 1.6\%$ for all cases).

Notably, more changes in thermal neutron flux shape and magnitude for ^{233}U case were observed in the inner core zone ($R \lesssim 150$) than in the outer core zone. In contrast, for Pu reactor-grade and TRU cases, significant changes were observed for thermal neutron flux in the outer core zone and reflector. Additionally, Figure 14 shows relatively large changes in thermal flux leakage from the core for the Pu and TRU cases. Overall, the SD-TMSR core design was optimized for ^{233}U fissile isotope [5]; thus, the core geometry (e.g., fuel channels lattice pitch) must be re-optimized for another type of fuel to obtain better

neutronics performance.

5.6. Temperature coefficient of reactivity

The temperature coefficient of reactivity quantifies reactivity changes due to temperature increase in the core and was calculated in this work as follows:

$$\alpha = \frac{k_{eff}(T_{i+1}) - k_{eff}(T_i)}{k_{eff}(T_{i+1})k_{eff}(T_i)(T_{i+1} - T_i)} \tag{2}$$

where

$$k_{eff} = \text{effective multiplication factor}$$

$$T_i = \text{fuel salt temperature in (900 K, 1000 K).}$$

Table 8 summarizes temperature coefficients calculated for three different initial fissile loads at the startup and at the equilibrium. By propagating the k_{eff} statistical error provided by SERPENT-2, uncertainty for each temperature coefficient was calculated using formula:

$$\delta\alpha = \left|\frac{1}{T_{i+1} - T_i}\right| \sqrt{\frac{\delta k_{eff}^2(T_{i+1})}{k_{eff}^4(T_{i+1})} + \frac{\delta k_{eff}^2(T_i)}{k_{eff}^4(T_i)}} \tag{3}$$

where

$$\delta k_{eff} = \text{statistical error for } k_{eff} \text{ from SERPENT-2 output.}$$

Notably, other sources of uncertainty are neglected, such as cross-section measurement error and approximations inherent in the density dependence on temperature.

When the fuel salt temperature increases, the density of the salt decreases, but at the same time, the total volume of fuel salt in the core remains constant because it is bounded by the vessel. When the graphite temperature increases, the density of graphite decreases, creating additional space for the salt. The cross-section temperatures for the fuel and moderator were changed from 900 to 1000 K to determine the temperature coefficients. This work considered five different cases:

1. Fuel salt temperature (Doppler Effect) rising from 900 to 1000 K (first row in Table 8).
2. Fuel salt density decreasing from 3.3 to 3.233 g/cm^3 (density change caused by temperature increase from 900 to 1000 K).
3. Total fuel salt temperature (Doppler+density) rising from 900 to 1000 K.
4. Graphite temperature (Doppler Effect) rising from 900 to 1000 K.
5. Whole reactor temperature rising from 900 K to 1000 K.

In the first case, the fuel temperature change only impacts cross-section temperature. In the second case, changes in the fuel temperature only impact density, and the third case takes into account both effects. The geometry for these three cases is unchanged because the fuel is a liquid. However, when the graphite blocks heat up, both the density and the geometry changing due to the thermal expansion of solid graphite. The graphite linear thermal expansion is not a dominating factor [5], and herein we focus only on Doppler Effect for the moderator temperature coefficient.

The Fuel Temperature Coefficient (FTC) is negative for all considered fuel compositions due to thermal Doppler broadening of the resonance capture cross-sections in the thorium. For ^{233}U case, the FTC decreases in magnitude by

Table 8: Temperature coefficients of reactivity for 3 different initial fuel salt compositions at startup and equilibrium. Confidence interval $\pm\sigma$ for all coefficients is between 0.11 and 0.16 pcm/K).

Reactivity coefficient (pcm/K)	Startup fissile material					
	^{233}U		Pu		TRU	
	Initial	Equil.	Initial	Equil.	Initial	Equil.
Fuel salt temperature	−4.96	−5.26	−4.99	−3.12	−3.23	−1.97
Fuel salt density	+1.49	+2.34	+1.54	−1.58	−0.37	−1.62
Total salt fuel	−3.77	−2.83	−3.22	−4.23	−3.25	−3.69
Graphite temperature	+1.45	+0.45	−2.68	−1.37	−1.44	−1.14
Total core	−1.77	−2.59	−6.54	−5.06	−4.79	−4.76

−25% due to neutron spectrum hardening during the reactor operation. For Pu reactor-grade and TRU cases, the FTC becomes more negative at the equilibrium, by +31% and +14%, respectively. Spectrum softening for these fueling cases positively affects the FTC magnitude, and this effect seems to be proportional to the spectrum shift.

The Moderator Temperature Coefficient (MTC) for the ^{233}U case is positive and decreases during reactor operation because of spectrum hardening with fuel depletion. For other cases, the MTC is negative and also decreasing in magnitude during the reactor operation. Finally, the total temperature coefficient of reactivity is strongly negative for all considered scenarios but decreases in magnitude during reactor operation due to spectral shift. Notably, the total temperature coefficient is the most negative for the Pu reactor-grade case at startup, which has the hardest neutron spectrum (Figure 12). These coefficients agree with earlier estimates for SD-TMSR [5, 29] and MSBR [7, 30, 20].

Even after 30 years of operation, the total temperature coefficient of reactivity remains relatively large and negative (in the range between −2.59 and −5.06 pcm/K) comparing with the conventional PWR, which has temperature coefficient of about $-1.71\ pcm/^{\circ}F \approx -3.08\ pcm/K$ [31]), and allows excellent reactor stability and control. The additional analysis must be performed taking graphite moderator density change and linear thermal expansion into account, but material properties for the SD-TMSR graphite are not available in published literature. Alternatively, relatively well-studied reactor graphite (e.g., AXQ graphite [20]) can be considered as a candidate for the SD-TMSR concept.

5.7. Six Factor analysis

The effective multiplication factor can be expressed as follows:

$$k_{eff} = k_{inf} P_f P_t = \eta f p \epsilon P_f P_t \tag{4}$$

where

$$\eta = \text{thermal fission factor}$$

$$f = \text{thermal utilization factor}$$

$$p = \text{resonance escape probability}$$

$$\epsilon = \text{fast fission factor}$$

$$P_f = \text{fast non-leakage probability}$$

$$P_t = \text{thermal non-leakage probability.}$$

Table 9 summarizes the six factors for 3 different initial fuel salt compositions at startup and equilibrium. By using SERPENT-2 built-in online reprocessing capabilities, all six factors have been calculated at the beginning of the operation and after 30 years of operation. Neutron population and number of active/inactive cycles were selected to obtain k_{eff} statistical uncertainty less than 12 pcm. The fast and thermal non-leakage probabilities remain constant regardless of initial fissile material and neutron spectrum shift during operation. The thermal utilization factor (f) remains almost constant during operation for ^{233}U and TRU cases but considerably declines for Pu case due to significant neutron spectrum softening.

Table 9: Six factors for the SD-TMSR model for 3 different initial fuel salt compositions at startup and equilibrium.

Factor	Startup fissile material					
	^{233}U		Pu		TRU	
	Initial	Equil	Initial	Equil	Initial	Equil
η	1.26	1.40	1.66	1.44	1.59	1.31
f	0.97	0.98	0.96	0.76	0.80	0.75
p	0.54	0.43	0.26	0.16	0.17	0.15
ϵ	1.49	1.67	2.45	5.87	4.83	6.81
P_f	0.99	0.99	0.99	0.99	0.99	0.99
P_t	1.00	1.00	1.00	1.00	1.00	1.00

In contrast, the neutron reproduction factor (η), resonance escape probability (p), and fast fission factor (ϵ) differ notably between initial and equilibrium state for all three initial fissile materials. The fast fission factor (ϵ) is much larger at startup for Pu and TRU cases because these initial fissile materials provided a much harder neutron spectrum than ^{233}U, and ϵ grows throughout the core's lifetime. Conversely, the resonance escape probability decreases during reactor operation. The thermal fission factor increases during reactor operation for the ^{233}U as initial fuel due to the accumulation of fissile plutonium isotopes, which produce more neutrons per fission (ν). The other two scenarios demonstrated opposite behavior: plutonium isotopes with large neutrons per fission production (ν) are gradually substituted with the ^{233}U, which has lower ν [32]. This six factors' evolution agrees with previously determined evolution parameters for a similar single-fluid double-zone MSBR [29, 7, 33].

6. Conclusion

In the present paper, five different types of initial fissile materials have been studied for transitioning to thorium fuel cycle in the SD-TMSR. The molar composition of start-up fuel for all five cases is listed in Table 4, as well, the inventories in Table 5. We adopted two different feed mechanisms; thorium feed mechanism and non-thorium feed mechanism. The whole-core of the SD-TMSR was simulated with Pu reactor-grade, TRU, and ^{233}U as initial fissile materials. Additionally, the variation of the effective multiplication factor k_{eff}, inventory, and other neutronic parameters have been investigated. Results demonstrated that continuous flow of Pu reactor-grade helps in transition to thorium fuel cycle within a relatively short time ($\approx 4.5\ years$) compared to 26 $years$ for Th/^{233}U start-up fuel. Meanwhile, using TRU as initial fissile materials shows the possibility of operating the SD-TMSR for a long period of time ($\approx 40\ years$) without any external feed of ^{233}U. in addition, the Pu proportion in fuel salt has been calculated and found to be below the solubility limit. Finally, the neutron spectrum shift during the reactor operation for the three selected cases has been

calculated.

7. Future work

8. Conflict of interest

The authors declare no conflict of interest.

9. Acknowledgments

Osama Ashraf would like to thank the Egyptian Ministry of Higher Education (MoHE), as well as MEPhI's Competitiveness Program for providing financial support for this research. The facility and tools needed to conduct this work were supported by MEPhI.

The authors contributed to this work as described below.

Osama Ashraf conceived and designed the simulations, wrote the paper, prepared figures and/or tables, performed the computation work, and reviewed drafts of the paper.

Andrei Rykhlevskii conceived and designed the simulations, wrote the paper, prepared figures and/or tables, performed the computation work, and reviewed drafts of the paper. Andrei Rykhlevskii is supported by DOE ARPA-E MEITNER program award DE-AR0000983.

G. V. Tikhomirov directed and supervised the work, conceived and designed the simulations and reviewed drafts of the paper. Prof. Tikhomirov is supported by Rosatom, he is Deputy Director of the Institute of Nuclear Physics and Engineering MEPhI. Board member of Nuclear society of Russia.

Kathryn D. Huff supervised the work, conceived and contributed to conception of the simulations, and reviewed drafts of the paper. Prof. Huff is supported by the Nuclear Regulatory Commission Faculty Development Program, the National Center for Supercomputing Applications, the NNSA Office of Defense Nuclear Nonproliferation R&D through the Consortium for Verfication Technologies and the Consortium for Nonproliferation Enabling Capabilities, the International

Institute for Carbon Neutral Energy Research (WPI-I2CNER), sponsored by the Japanese Ministry of Education, Culture, Sports, Science and Technology, and DOE ARPA-E MEITNER program award DE-AR0000983.

This research is part of the Blue Waters sustained-petascale computing project, which is supported by the National Science Foundation (awards OCI-0725070 and ACI-1238993) and the state of Illinois. Blue Waters is a joint effort of the University of Illinois at Urbana-Champaign and its National Center for Supercomputing Applications

References

[1] DOE, US, A technology roadmap for generation iv nuclear energy systems (2002) 48–52.

[2] D. D. Siemer, Why the molten salt fast reactor (msfr) is the best gen iv reactor, Energy Science & Engineering 3 (2) (2015) 83–97.

[3] M. Rosenthal, P. Kasten, R. Briggs, Molten-salt reactorshistory, status, and potential, Nuclear Applications and Technology 8 (2) (1970) 107–117.

[4] I. Pioro, Handbook of generation IV nuclear reactors, Woodhead Publishing, 2016.

[5] G. C. Li, P. Cong, C. G. Yu, Y. Zou, J. Y. Sun, J. G. Chen, H. J. Xu, Optimization of Th-U fuel breeding based on a single-fluid double-zone thorium molten salt reactor, Progress in Nuclear Energy 108 (2018) 144–151. doi:10.1016/j.pnucene.2018.04.017.
URL http://www.sciencedirect.com/science/article/pii/S0149197018300970

[6] A. Nuttin, D. Heuer, A. Billebaud, R. Brissot, C. Le Brun, E. Liatard, J.-M. Loiseaux, L. Mathieu, O. Meplan, E. Merle-Lucotte, et al., Potential of thorium molten salt reactorsdetailed calculations and concept evolution with a view to large scale energy production, Progress in nuclear energy 46 (1) (2005) 77–99.

[7] A. Rykhlevskii, J. W. Bae, K. D. Huff, Modeling and simulation of online reprocessing in the thorium-fueled molten salt breeder reactor, Annals of Nuclear Energy 128 (2019) 366–379. doi:10.1016/j.anucene.2019.01.030.

[8] E. Merle-Lucotte, D. Heuer, C. Le Brun, J. Loiseaux, Scenarios for a worldwide deployment of nuclear energy production.

[9] B. R. Betzler, J. J. Powers, A. Worrall, Modeling and simulation of the start-up of a thorium-based molten salt reactor, in: Proc. Int. Conf. PHYSOR, 2016.

[10] C. Zou, C. Cai, C. Yu, J. Wu, J. Chen, Transition to thorium fuel cycle for tmsr, Nuclear Engineering and Design 330 (2018) 420–428.

[11] C. Zou, G. Zhu, C. Yu, Y. Zou, J. Chen, Preliminary study on trus utilization in a small modular th-based molten salt reactor (smtmsr), Nuclear Engineering and Design 339 (2018) 75–82.

[12] D. Heuer, E. Merle-Lucotte, M. Allibert, M. Brovchenko, V. Ghetta, P. Rubiolo, Towards the thorium fuel cycle with molten salt fast reactors, Annals of Nuclear Energy 64 (2014) 421–429.

[13] O. Ashraf, A. Smirnov, G. Tikhomirov, Modeling and criticality calculation of the molten salt fast reactor using serpent code, in: Journal of Physics: Conference Series, Vol. 1189, IOP Publishing, 2019, p. 012007.

[14] O. Ashraf, A. Smirnov, G. Tikhomirov, Nuclear fuel optimization for molten salt fast reactor, in: Journal of Physics: Conference Series, Vol. 1133, IOP Publishing, 2018, p. 012026. doi:doi:10.1088/1742-6596/1133/1/012026.

[15] C. Fiorina, M. Aufiero, A. Cammi, F. Franceschini, J. Krepel, L. Luzzi, K. Mikityuk, M. E. Ricotti, Investigation of the msfr core physics and fuel cycle characteristics, Progress in Nuclear Energy 68 (2013) 153–168.

[16] C. de Saint Jean, M. Delpech, J. Tommasi, G. Youinou, P. Bourdot, Scénarios cne: réacteurs classiques, caractérisation à l'équilibre, rapport CEA DER/SPRC/LEDC/99-448.

[17] M. Jiang, H. Xu, Z. Dai, Advanced fission energy program-tmsr nuclear energy system, Bull. Chin. Acad. Sci 27 (3) (2012) 366–374.

[18] X. Li, X. Cai, D. Jiang, Y. Ma, J. Huang, C. Zou, C. Yu, J. Han, J. Chen, Analysis of thorium and uranium based nuclear fuel options in fluoride salt-cooled high-temperature reactor, Progress in Nuclear Energy 78 (2015) 285–290.

[19] G. Li, Y. Zou, C. Yu, et al., Model optimization and analysis of th–u breeding based on msfr, Nucl. Tech 40 (2017) 020603–020603.

[20] R. C. Robertson, Conceptual Design Study of a Single-Fluid Molten-Salt Breeder Reactor., Tech. Rep. ORNL–4541, comp.; Oak Ridge National Laboratory, Tenn. (Jan. 1971).
URL http://www.osti.gov/scitech/biblio/4030941

[21] J. C. Marka, Explosive properties of reactor-grade plutonium, Science & Global Security 4 (1) (1993) 111–128.

[22] N. OECD, Probabilistic safety assessment in nuclear power plant management: a report by a group of experts of the nea committee on the safety of nuclear installations, june 1989, 112 (1989).

[23] J. Serp, M. Allibert, O. Beneš, S. Delpech, O. Feynberg, V. Ghetta, D. Heuer, D. Holcomb, V. Ignatiev, J. L. Kloosterman, et al., The molten salt reactor (msr) in generation iv: overview and perspectives, Progress in Nuclear Energy 77 (2014) 308–319.

[24] J. Leppänen, M. Pusa, T. Viitanen, V. Valtavirta, T. Kaltiaisenaho, The serpent monte carlo code: Status, development and applications in 2013, in: SNA+ MC 2013-Joint International Conference on Supercomputing in Nuclear Applications+ Monte Carlo, EDP Sciences, 2014, p. 06021.

[25] M. Aufiero, A. Cammi, C. Fiorina, J. Leppänen, L. Luzzi, M. E. Ricotti, An extended version of the serpent-2 code to investigate fuel burn-up and core material evolution of the molten salt fast reactor, Journal of Nuclear Materials 441 (1-3) (2013) 473–486.

[26] A. Isotalo, M. Pusa, Improving the accuracy of the chebyshev rational approximation method using substeps, Nuclear Science and Engineering 183 (1) (2016) 65–77.

[27] V. Ignatiev, O. Feynberg, A. Merzlyakov, A. Surenkov, A. Zagnitko, V. Afonichkin, A. Bovet, V. Khokhlov, V. Subbotin, R. Fazilov, et al., Progress in development of mosart concept with th support, in: Proceedings of ICAPP, Vol. 12394, 2012.

[28] D. Sood, P. Iyer, R. Prasad, V. Vaidya, K. Roy, V. Venugopal, Z. Singh, M. Ramaniah, Plutonium trifluoride as a fuel for molten salt reactors-solubility studies, Nuclear technology 27 (3) (1975) 411–415.

[29] O. Ashraf, A. Rykhlevskii, G. Tikhomirov, K. D. Huff, Whole core analysis of the single-fluid double-zone thorium molten salt reactor (sd-tmsr), Annals of Nuclear Energy.

[30] A. Rykhlevskii, A. Lindsay, K. D. Huff, Full-core analysis of thorium-fueled Molten Salt Breeder Reactor using the SERPENT 2 Monte Carlo code, in: Transactions of the American Nuclear Society, American Nuclear Society, Washington, DC, United States, 2017.

[31] B. Forget, K. Smith, S. Kumar, M. Rathbun, J. Liang, Integral Full Core Multi-Physics PWR Benchmark with Measured Data, Tech. rep., Massachusetts Institute of Technology (2018).

[32] N. G. Sjöstrand, J. S. Story, Cross sections and neutron yields for U-233, U-235 and Pu-239 at 2200 m/sec, Tech. rep., AB Atomenergi (1960).

[33] J. Park, Y. Jeong, H. C. Lee, D. Lee, Whole core analysis of molten salt breeder reactor with online fuel reprocessing, International Journal of Energy

Research 39 (12) (2015) 1673–1680. doi:10.1002/er.3371.
URL http://doi.wiley.com/10.1002/er.3371